

Competition between Electron-Phonon coupling and Spin Fluctuations in superconducting hole-doped BiOCuS

Luciano Ortenzi,¹ Silke Biermann,² Ole Krogh Andersen,¹ I.I. Mazin,³ and Lilia Boeri¹

¹*Max-Planck-Institut für Festkörperforschung, Heisenbergstraße 1, D-70569 Stuttgart, Germany*

²*Centre de Physique Théorique, Ecole Polytechnique, CNRS-UMR7644, 91128 Palaiseau, France*

³*Naval Research Laboratory, 4555 Overlook Avenue SW, Washington, DC 20375, USA*

(Dated: October 18, 2018)

BiOCuS is a band insulator that becomes metallic upon hole doping. Superconductivity was recently reported in doped BiOCu_{1-x}S and attributed to spin fluctuations as a pairing mechanism. Based on first principles calculations of the electron-phonon coupling, we argue that the latter is very strong in this material, and probably drives superconductivity, which is however strongly depressed by the proximity to magnetism. We find however that BiOCu_{1-x}S is a quite unique compound where both a conventional phonon-driven and an unconventional triplet superconductivity are possible, and compete with each other. We argue that, in this material, it should be possible to switch from conventional to unconventional superconductivity by varying such parameters as doping or pressure.

PACS numbers: 63.20.Kd, 74.20.Pq, 74.20.Mn, 74.70.Xa

The study of spin fluctuations as superconducting mediators dates back to the sixties;^{1,2} however, in contrast to the electron-phonon (EP) interaction, for which a detailed first-principles theory has been developed in the last twenty years, a quantitative theory is still lacking. In several materials where at some point ferromagnetic spin fluctuations (paramagnons) were considered as potential pairing agents, such as ZrZn₂,³ MgCNi₃,⁴ or Pd metal,¹ phonon and spin fluctuations contributions either cancel, rendering the material non-superconducting (ZrZn₂, Pd), or the latter substantially decreases the superconducting transition temperature.

Recently, superconductivity with $T_c=5.8$ K has been discovered in hole-doped BiOCu_{0.9}S.⁵ BiOCuS crystallizes in the *ZrCuAsSi*-type structure, isostructural to the 1111-family of Fe-based superconductors, with Cu-S layers playing the role of Fe-As layers. While Cu-S hybridized *dp* bands *per se* are rather similar to the Fe-As bands in Fe-pnictides, the different electronic filling brings about very different properties in the two systems. The stoichiometric BiOCuS is in fact a band insulator with the Cu being in the d^{10} electronic configuration.⁵⁻⁷ With hole-doping it displays both a strong tendency to itinerant (ferro)magnetism, and a spectacularly strong EP coupling, hinting to unconventional, triplet *p*-wave,⁸ and conventional, singlet *s*-wave superconductivity, respectively.

In this paper, we study the interplay between these competing instabilities, using first-principles calculations of BiOCu_{1-x}S as a function of doping and Stoner parameter, which we use as a proxy for the tendency to magnetism. We find that, as the EP coupling is spectacularly strong, it is likely that a conventional superconductivity, even though depressed by spin fluctuations, is more stable than an unconventional (*e.g.* *p*-wave) one. It appears though that a small variation of parameters can reverse the situation and bring triplet superconductivity or long-range magnetism. We identify two large regions in the parameter space where, respectively, ferromagnetism

(FM) or conventional *s*-wave superconductivity are the ground states, with an intermediate region where no FM long range order is predicted, yet spin fluctuations are strong enough to destroy the *s*-wave superconductivity and possibly stabilize a triplet state.

We perform calculations in the linear-response approximation for the EP interaction, and in the local spin density functional version of the random-phase approximation (RPA) for spin fluctuations, as described below; doping is treated in the rigid band approximation (RBA).⁹

The generalized-gradient approximation (GGA) band structure and partial electronic density of states (DOS) are shown in Fig. 1; in agreement with previous calculations,^{5,8,15} we find that the stoichiometric compound is a semiconductor^{5,6} with an indirect gap of $\Delta \approx 0.5$ eV (GGA); the top of the valence band occurs along the $\Gamma - M$ line, and we choose it as the zero of the energy in the following. The electronic structure in an energy range ~ 7 eV below the top of the valence band in BiOCuS is derived from Cu *d* and S *p* states (see top panel of Fig. 1). The Cu *d* states are centered around ~ -2 eV. They hybridize strongly with the S *p* states, forming anti-bonding bands within ~ 1 eV below the semiconducting gap. The EP matrix element is large for these bands, as the electronic states are very sensitive to ionic displacements. On the contrary, the deeper, non-bonding, Cu *d* bands, centered around ~ -3 eV, are less sensitive to the Cu-S hopping parameters and exhibit a much weaker EP interaction. The tendency to magnetism is instead strong throughout the entire Cu *d* band, since the Stoner parameter of Cu is large ($I_{Cu} \approx 0.9$ eV).

In pure BiOCuS, Cu is in a nominal d^{10} state and thus not magnetic. Doping with holes, for $x \leq 0.5$, shifts the Fermi level into a doubly-degenerate band, with dominant Cu d_{xz} , d_{yz} and S p_x , p_y characters and large DOS. The bottom panel of Fig. 1 shows a blow-up of the band structure in the energy range relevant for superconductivity. The dotted and dashed lines indicate respectively the position of the Fermi level for $x = 0.1$, corresponding

to the doping for which superconductivity was observed in Ref. 5, and $x = 0.5$, which is the highest doping considered in our RBA study.

If we could shift the Fermi level further down, so as to cut the band structure at ~ -1.4 eV (dash-dotted line in the top panel of Fig. 1), we would find a striking similarity with the familiar low-energy electronic structure of Fe-pnictides, with the xz, yz hole and electron pockets, centered at Γ and M respectively. The DOS and the $p-d$ hybridization here are small, thus the tendency to antiferro- (rather than ferro-) magnetism, and low EP interaction. This is indeed what first-principles calculations find in Fe-pnictides.¹⁶

We now go back to discuss the behavior of $\text{BiOCu}_{1-x}\text{S}$ for $x \leq 0.5$, using the bottom panel of Fig. 1. For $x \geq 0.1$, we find the ground state of the system is FM, both in the local spin density approximation (LSDA) and in the GGA.⁸ This can be understood in terms of the Stoner criterion for FM, $IN_0 > 1$. When holes are introduced into the system, and the Cu charge state is being reduced from d^{10} to d^9 , the Fermi level moves into a flat region of the band structure, which gives rise to a high peak in the DOS ($N_0 = 2.1$ st/eV spin). Since the Stoner parameter of atomic Cu is $I_{\text{Cu}} \approx 0.9$ eV, the latter value of the DOS is well above the Stoner criterion for FM, $IN_0 > 1$. In $\text{BiOCu}_{1-x}\text{S}$ the actual value of $I \leq I_{\text{Cu}}$, due to the Cu-S hybridization. It can be estimated from the splitting $\Delta E = mI$ between majority and minority bands in the FM state, where m is the value of the self-consistent magnetic moment. We find $m \lesssim 0.1$ for all dopings considered, and $I = 0.53$ eV in LSDA and $I = 0.67$ eV in GGA, independent of doping. So far, however, experiments have seen no trace of static magnetism; this is consistent with the tendency of LSDA calculations to overestimate the tendency to itinerant magnetism with respect to experiment in the vicinity of a magnetic quantum critical point (QCP), where the system exhibits strong spin fluctuations.¹⁷ We will return to this issue in more detail, after discussing the results for the EP interaction.

Fig. 2 summarizes the EP properties of the hole-doped $\text{BiOCu}_{1-x}\text{S}$. The partial phonon density of states (PDOS) of the undoped compound extends up to 65 meV; vibrations of the Bi-O layers are concentrated at energies ≤ 20 meV, while modes involving the Cu-S layers are found at higher energies. The S atoms give rise to a very broad feature in the PDOS, from 40 to 65 meV. Using this phonon spectrum, we calculate the Eliashberg spectral function $\alpha^2 F(\omega)$ of the hole-doped $\text{BiOCu}_{1-x}\text{S}$:

$$\alpha^2 F(\omega) = \frac{1}{N_0} \sum_{\mathbf{k}, \mathbf{q}, \nu, n, m} \delta(\epsilon_{\mathbf{k}}^n) \delta(\epsilon_{\mathbf{k}+\mathbf{q}}^m) |g_{\mathbf{k}, \mathbf{k}+\mathbf{q}}^{\nu, n, m}|^2 \delta(\omega - \omega_{\nu \mathbf{q}}),$$

evaluating the average of the EP matrix elements $g_{\mathbf{k}, \mathbf{k}+\mathbf{q}}^{\nu, n, m}$ on the Fermi surface $\delta(\epsilon_{\mathbf{k}}^n)$, obtained by a rigid-band shift corresponding to the doping level. From the Eliashberg function we calculate the EP coupling constant:

$$\lambda_{\text{ep}} = 2 \int_0^\infty d\Omega \alpha^2 F(\Omega) / \Omega.$$

For all dopings $x \leq 0.5$, we find that only two groups of

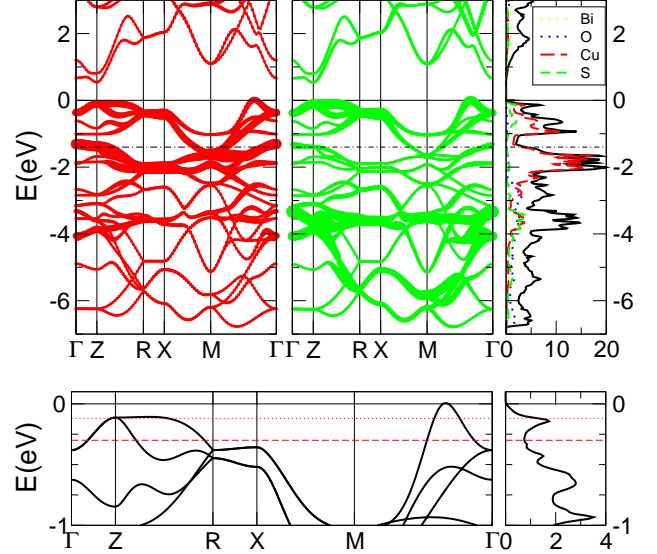


FIG. 1: (color online). *top* Band structure of BiOCuS , shaded according to the partial Cu d_{xz+yz} (left) and S p_{x+y} (right) characters: the continuous and dashed-dotted lines mark respectively the position of the Fermi level in the undoped compound and that corresponding to the filling d^6 of Fe-pnictides (see text); the corresponding DOS is also shown. *bottom*: a blow-up of the low-energy band structure; the dashed and dotted line mark the position of the Fermi level, corresponding to a hole doping $x = 0.1$ and $x = 0.5$, in RBA.

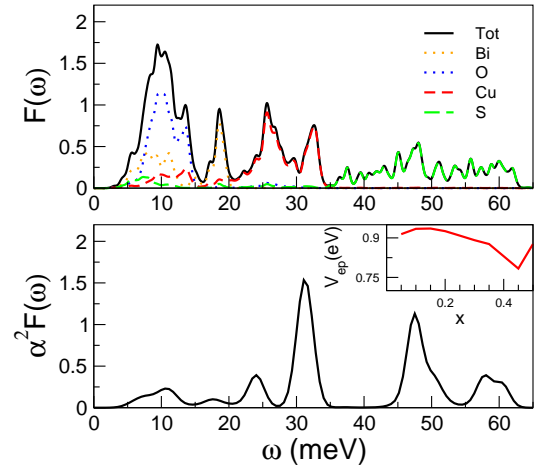


FIG. 2: (color online). From top to bottom: Partial Phonon density of States (PDOS), Eliashberg spectral function for $x = 0.1$, in RBA, and (inset) ratio between the coupling constant and the DOS as a function of doping.

phonon modes, corresponding to the out-of-plane vibrations of the Cu-S layers, have sizable EP matrix elements $g_{\mathbf{k}, \mathbf{k}+\mathbf{q}}^{\nu, n, m}$: these give rise to two narrow peaks in $\alpha^2 F(\omega)$, centered at 33 meV and 50 meV. The lower panel of Fig. 2 shows an example of $\alpha^2 F(\omega)$ for $x = 0.1$.

Since the shape of the Eliashberg function does not

depend on x for all dopings considered, the total EP coupling depends on doping only through the value of the density of states at the Fermi level, N_0 . We thus rewrite λ_{ep} as $\lambda_{\text{ep}} = N_0 V_{\text{ep}}$. As the inset of Fig. 2 shows, $V_{\text{ep}} \simeq 0.9$ eV spin f.u. at all dopings for $x \leq 0.5$. For comparison, $V_{\text{ep}} = 0.1$ eV spin f.u. in LaOFeAs and $V_{\text{ep}} = 0.3$ eV spin f.u. in Pd (*i.e.* in metals where the lattice plays a minor role compared to spin fluctuations) while it is much larger in good EP superconductors: $V_{\text{ep}} = 2.5$ eV spin f.u. in MgB₂ or $V_{\text{ep}} = 6.6$ eV spin f.u. in Pb.

For $x = 0.1$, $N_0 = 1.93$ st/eV spin f.u., $\lambda_{\text{ep}} = 1.74$ and the logarithmically averaged phonon frequency $\omega_{\text{log}} = 263$ K. This EP interaction would then give rise to a T_c of 33 K, assuming a typical value for the Coulomb pseudopotential, $\mu^* = 0.1$.

This is much larger than the experimental value $T_c = 5.8$ K,⁵ which would correspond to $\lambda_{\text{ep}} = 0.6$.¹⁸ A factor three discrepancy is well above the typical uncertainty of T_c in similar calculations, stemming from the computational uncertainty on λ_{ep} , typically 10%, or from the uncertainty of μ^* .

The most straightforward explanation, in the present case, is a suppression of phonon-mediated pairing by strong paramagnons, due to proximity to a FM QCP. We now estimate this effect, using the RPA. Let λ_{sf}^s be the coupling to spin fluctuations in the singlet channel; the effect of paramagnons is to suppress superconductivity in the singlet channel by depressing the effective coupling constant ($\lambda_{\Delta} = \lambda_{\text{ep}} - \lambda_{\text{sf}}^s$) and increasing the effective mass of the carriers by the factor $1 + \lambda_Z = 1 + \lambda_{\text{ep}} + \lambda_{\text{sf}}^s$. This effect has been studied in Ref. 19 where the following expression for T_c was derived (and verified by comparison with numerical solutions of the Eliashberg equations):

$$T_c = \frac{\omega_{\text{log}}}{1.45} \exp \left\{ \frac{-(1 + \lambda_Z)}{\lambda_{\Delta} - \mu^*(1 + 0.5 \frac{\lambda_{\Delta}}{1 + \lambda_Z})} \right\}. \quad (1)$$

Here we assume for simplicity that the characteristic frequencies of phonons and electrons are the same. Eq. 1 can also be generalized to triplet superconductivity, with the substitution: $\lambda_{\Delta} \rightarrow \lambda_{\text{sf}}^t$; $\lambda_Z \rightarrow \lambda_Z^t = \lambda_{\text{ep}} + \lambda_{\text{sf}}^t$, where $\lambda_{\text{sf}}^t = \frac{1}{3} \lambda_{\text{sf}}^s$ is the coupling to spin fluctuations in the triplet channel.²⁰ Eq. 1 gives an appreciable T_c only if the denominator in the exponential is positive. For small μ^* , this is the case, when $\lambda_{\Delta} > 0$. We therefore use λ_{Δ} to define the phase diagram of hole-doped BiOCu_{1-x}S: using the RBA, we take $\lambda_{\text{ep}}(x) = V_{\text{ep}} N_0(x)$, where $N_0(x)$ is the DOS at the Fermi level at doping x . For the coupling to spin fluctuations we use the following expression:

$$\lambda_{\text{sf}}^s(x) = \frac{3}{2} \frac{N_0^2(x) I^2}{1 - I N_0(x)} \quad (2)$$

where I is, in the LDA parlance, the Stoner parameter.²¹ Eq. 2 is similar to the well-known expression for the spin fluctuations induced interaction in the singlet channel,²⁰ averaged over the Fermi surface. Note that in the triplet channel the spin fluctuations interaction is three times

smaller, and also the averaging for both λ_{sf} and λ_{ep} is performed with a weighting factor $\hat{v}_F(\mathbf{k}) \cdot \hat{v}_F(\mathbf{k}')$.

A well-known LDA problem is that, due to its mean-field character, it overestimates the tendency to static magnetism.²² This can be corrected by introducing a phenomenological Stoner I , reduced from its LDA value. In this spirit, in the following, we treat I as a free parameter, and plot the phase diagram of BiOCuS in the (x, I) space. The results are shown in Fig. 3.

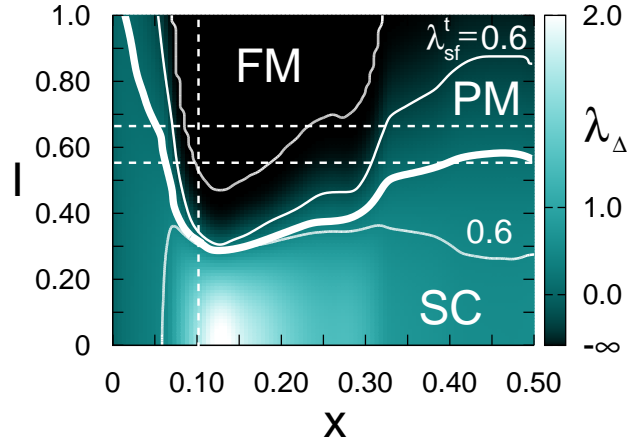


FIG. 3: (color online). Phase diagram of BiOCu_{1-x}S, defined by λ_{Δ} as a function of doping (x) and Stoner parameter I , whose value is represented by the color scale. The two horizontal dashed lines correspond to $I_{\text{LDA}} = 0.53$ eV and $I_{\text{GGA}} = 0.67$ eV. The vertical dashed line indicates the doping for which superconductivity was observed in Ref. 5. In the region (FM) the system shows a FM instability, defined by the condition ($N_0 I \geq 1$); elsewhere the system is paramagnetic (PM). Below the bold line (which marks the condition $T_c^s = T_c^t$) the ground state is a conventional singlet superconductor. Above the bold line a triplet superconducting state is more stable. The isolines $\lambda_{\Delta} = 0.6$ and $\lambda_{\text{sf}}^t = 0.6$ indicate the values of I, x which reproduce the experimental $T_c = 5.8$ K of Ref. 5 in the singlet and triplet channel respectively.

If $\lambda_{\Delta} \gg \mu^*$ a conventional EP superconductivity, albeit depressed by spin fluctuations, is a stable zero-temperature ground state. As the Stoner parameter is increased λ_{Δ} goes down, and a competing instability against a triplet state emerges when the critical temperature in the singlet channel T_c^s , defined by Eq. 1, becomes equal to that in the triplet channel (T_c^t). Finally, as the tendency to magnetism is increased even further, the Stoner criterion $N_0 I > 1$ is satisfied, and the system becomes ferromagnetic (Fig. 3).

One can see that, had we used the LDA or GGA value for I , for dopings close to $x = 0.1$, we would have found BiOCuS inside the FM region. However, at $x = 0.1$ experiments see no trace of static FM order, a sign of inadequacy of the mean field character of magnetism in LSDA. Reducing the LDA value of I to $I_{\text{eff}} = 0.51$ eV suppresses the magnetic instability at $x = 0.1$; a reduction to $I_{\text{eff}} = 0.39$ eV brings the estimated triplet T_c into agreement with the experimental one, and a reduction

to 0.25 eV does the same with the conventional singlet T_c . For typical itinerant magnets renormalizing I_{LDA} by $\sim 30 - 40\%$ provides reasonable agreement with the experimental magnetic susceptibilities,²² in the same ballpark as the reduction introduced above.

In other words, $\text{BiOCu}_{0.9}\text{S}$ is a unique example where a spin fluctuations driven triplet superconductivity is nearly degenerate with the phonon-driven singlet superconductivity, and the critical temperature is sizable for both symmetries. Given that the actual $\text{BiOCu}_{0.9}\text{S}$ samples are rather dirty, one may conjecture that samples studied in Ref. 5 are on the conventional side of the phase diagram, but the fact that superconductivity appears to be so difficult to reproduce may be due to the fact that slightly different samples may appear outside of the stability range of singlet pairing in the phase diagram in Fig. 3. In principle, one can use pressure and doping, which control I and N_0 respectively, to move around intentionally in the proposed phase diagram.

This tunability comes about because of the combination of two factors: an exceptionally strong EP inter-

action in the singlet channel that is essentially canceled out in the triplet channel, and a strong spin fluctuations coupling that competes with EP interaction in the singlet channel. The occurrence of these two large coupling constants can be seen as the result of three concurring elements: a strong $d-p$ hybridization, that causes large EP matrix elements; the large value of the Stoner parameter of Cu, that causes a strong tendency to magnetism; and, finally, the presence of a large peak in the electronic DOS, which favors FM and enhances the coupling constants for superconductivity both in the singlet and triplet channel.

Acknowledgements: The authors would like to thank D. J. Scalapino, D. van der Marel and E. Giannini for useful discussions, and M. Calandra for help in developing the rigid-band routine. O.K.A. and S.B. acknowledge also the hospitality of KITP Santa Barbara, where this work was started. This research was supported in part by the National Science Foundation under Grant No. PHY05-51164, the French ANR under project Correlmat and IDRIS/GENCI under project 101393.

¹ N. F. Berk and J. R. Schrieffer, Phys. Rev. Lett. **17**, 433 (1966).

² D. Fay, J. Appel, Phys. Rev. B **22**, 3173 (1980).

³ G. Santi, S. B. Dugdale, and T. Jarlborg, Phys. Rev. Lett. **87**, 247004 (2001); I. I. Mazin and D. J. Singh, Phys. Rev. B **69**, 020402(R) (2004).

⁴ H. Rosner, *et al*, Phys. Rev. Lett. **88**, 027001 (2001); D. J. Singh and I. I. Mazin, Phys. Rev. B **64**, 140507(R) (2001); A. Yu. Ignatov, S. Y. Savrasov, and T. A. Tyson, Phys. Rev. B **68**, 220504(R) (2003).

⁵ A. Ubaldini, E. Giannini, C. Senatore, D. van der Marel, Physica C **470**, S356-S357 (2010).

⁶ H. Hiramatsu, *et al*, Chem. Mater. **20**, 326 (2008).

⁷ A. Pal, H. Kishan and V.P.S. Awana, J. Supercond. Novel Magn. **23**, 301 (2010).

⁸ I.I. Mazin, Phys. Rev. B **81**, 140508(R) (2010).

⁹ We use the experimental crystal structure, $a=3.8726$ Å and $c=8.5878$ Å, $z_{\text{Bi}}=0.14829$, $z_{\text{S}}=0.671$.^{5,6} For the band structure and DOS calculations, we employ the linearly augmented plane wave methods, as implemented in the Wien2K code.¹⁰ The linear response EP calculations are performed in the generalized gradient approximation¹¹ using plane-waves¹², ultra-soft¹³ and norm-conserving Martin-Trouillers¹⁴ pseudopotentials. We employ a cut-off of 100 (800) Ryd for the wave-functions (charge densities) and $4 \times 4 \times 2$ \mathbf{k} -mesh for the self-consistent cycles, Finer grids ($48 \times 48 \times 24$) are used for evaluating the EP linewidths, and the densities of states (DOS) in the doped regime. Dynamical matrices and EP linewidths are calculated on a $8 \times 8 \times 2$ uniform grid in \mathbf{q} -space. Phonon frequencies throughout the Brillouin Zone are obtained by Fourier interpolation. The (perturbed) potentials and charge densities, as well as the phonon frequen-

cies, are calculated self-consistently at zero doping ($x=0$); the effect of doping on the EP coupling was then estimated using RBA.

¹⁰ <http://www.wien2k.at>.

¹¹ J. P. Perdew, K. Burke, and M. Ernzerhof, Phys. Rev. Lett. **78**, 1396 (1997).

¹² P. Giannozzi *et al.*, <http://www.quantum-espresso.org>.

¹³ D. Vanderbilt, Phys. Rev. B **41**, R7892 (1990).

¹⁴ N. Trouiller and J.L. Martins, Phys. Rev. B **43**, 1991, (1993).

¹⁵ I. R. Shein and A. L. Ivanovskii, Solid State Commun. **150**, 640 (2010).

¹⁶ L. Boeri, *et al.*, Phys. Rev. B **82**, 020506 (2010).

¹⁷ "Density Functional Calculations near Ferromagnetic Quantum Critical Points", I. I. Mazin, D.J. Singh, and A. Aguayo, in Proceedings of the NATO ARW on Physics of Spin in Solids: Materials, Methods and Applications, ed. S. Halilov, Kluwer, 2004.

¹⁸ The values of T_c are obtained using Eq. 1, with $\lambda_{\text{sf}}^{\text{s}} = 0$. Using the Mc-Millan formula gives differences of less than 1K in T_c .

¹⁹ O. V. Dolgov, *et al*, Phys. Rev. Lett. **95**, 257003 (2005).

²⁰ D. J. Scalapino J. Low Temp. Phys. **117**, 179 (1999)

²¹ In BiOCuS , the LDA spin susceptibility has a large peak at $\mathbf{q} = 0$, due to intraband processes, and four smaller peaks at $\bar{\mathbf{q}} \sim (\pi/8, \pi/8)$, due to interband transitions; the relative weight is such that $\chi_0(\mathbf{0}, 0) \approx 2\chi_0(\bar{\mathbf{q}}, 0)$. Near the instability it is reasonable to keep only the contribution at $\mathbf{q} = 0$; in the $\omega = 0$ limit we obtain Eq. (2).

²² P. Larson, I. I. Mazin, and D. J. Singh, Phys Rev. B **69**, 064429 (2004); arXiv:cond-mat/0401563.